

Report: Commissioning Run: March 9-14, 2011
Debra Fischer, Matt Giguere
Yale University

The e2v-4K CCD and Monsoon Orange controller were returned to CTIO on March 9, 2011 and installed by A. Tokovinin and M. Bonati, the same day that Fischer and Giguere arrived.

Goals for this run included (1) testing of the detector, controller and spectrometer, (2) software development and (3) science tests. There are many possible configurations for the detector and our reduction scripts are currently only supporting the following:

1. Narrow slit: 3x1 binning, full chip, fast readout, resolution of 120,000
2. Slicer: 3x1 binning, full chip, fast readout, resolution of 90,000
3. Slit: 3x1 binning, full chip, fast readout, resolution of 90,000
4. Fiber: 3x1 binning, full chip, fast readout, resolution of 28,000

The full chip is read out in dual amp, fast read out mode in 14 seconds. While it is possible to window down the CCD frame, this does not save any readout time and adds more variables to the raw reduction script. Therefore, we trim the image in software, discarding orders with low flux that are more difficult to trace and extract. All spectra for Mar 9 – 14 have been reduced (extracted) and wavelength calibrated. All iodine spectra have been run through the Doppler code to analyze the LSF.

Technical Assessments

Here we comment on focus, tilt, rotation, pressure, temperature, throughput, resolution, and overall stability of the system.

Focus, tilt, rotation

All programs for checking tilt, focus and rotation are on *ctimac1* in */mir7/focus_ctio*. Using *fwhm_thar.pro*, we measured a FWHM of 2.3 pixels for the narrow slit mode. Using *rotate_ccd.pro* we checked positions for two identical lines in wrapped orders and found an acceptable difference of only 4 pixels (with about 2800 pixel separation).

Pressure

On the first day we attempted to measure the leakage rate from CHIRON. Andrei drilled a hole in a side panel of the enclosure (and insulation). The hole was located beneath the OSS so that injected air would not blow directly on the optics. The brass input pressure tap (built by Andy Szymkowiak, see **Figure 2**) was mounted with O-rings and nuts. The pressure sensor was placed inside and at the top front of the enclosure with the power cord running through a break in the rubber seal to connect to a laptop.

If we do seal the enclosure, then we will need a pressure sensor with better precision. However, an attractive option for CHIRON is replacing the current grating with a new (higher efficiency) grating in vacuum.

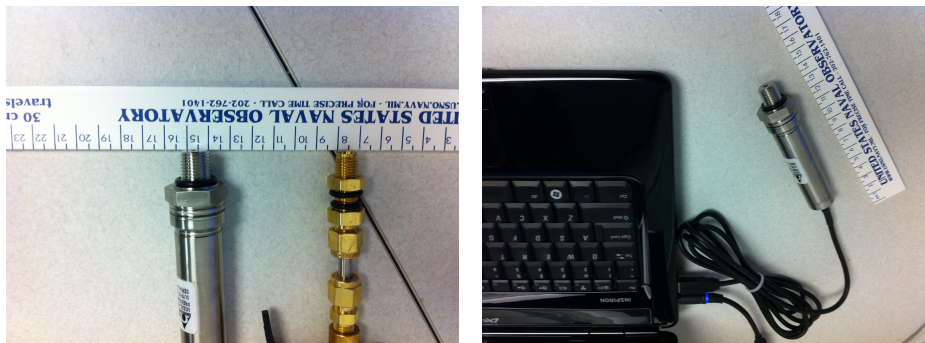


Figure 2. (left) the iOmega pressure sensor and input tap for the enclosure. (right) pressure sensor with cord, which connects to laptop for monitoring.

We initially used the N_2 tank to provide gas to fill the enclosure, being careful to monitor the line for the presence of liquid nitrogen. This resulted in an increase of only 0.3 mbar in the pressure (**Figure 3, left**) and we were not able to even sustain this pressure because we depleted the gaseous N_2 and liquid began coming out of the tank. The pressure dropped back to the baseline value about two seconds after the N_2 flow was turned off. We then tried using an air compressor to overpressure the enclosure. The air compressor produced a gentle flow of air, but the flow rate was not sufficient to increase pressure inside the enclosure. The enclosure is clearly not very tight and pressure measurements through the night (**Figure 3, right**) show variations of about 3 mbar over 24 hours.

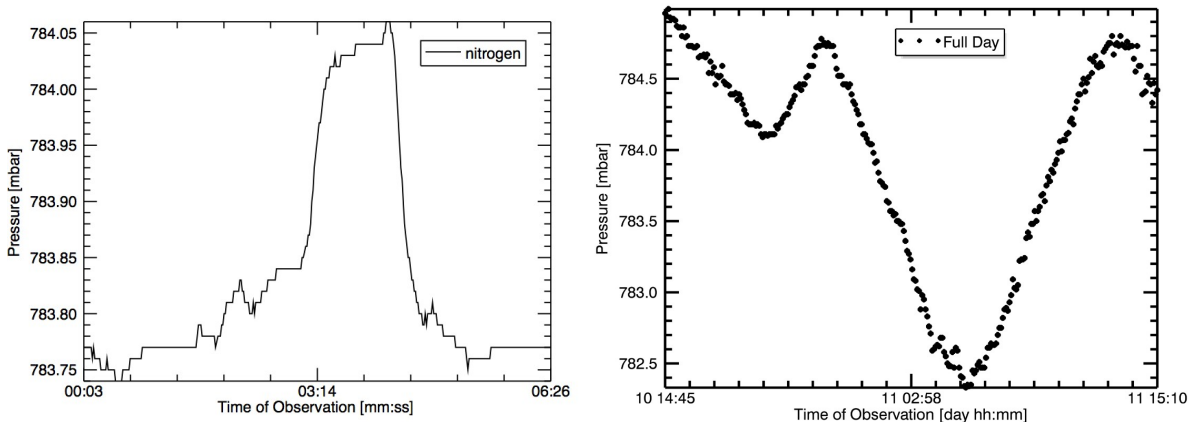


Figure 3. (left) Plot of the change in pressure measured by the sensor when gaseous N_2 was used as a source for overpressure. The time decay occurred in about two seconds. (right) pressure was passively monitored and varied by about 3 mbar over 24 hours.

Temperature

Temperature is monitored in the Coude room, the iodine cell and at three points inside the spectrograph enclosure (**Figure 4**). The CHIRON enclosure is heated and shows temperature variations with rms $\sim 0.1K$. There is a heating unit in the Coude room with a thermostat, however large temperature cycling is still observed. A tent will soon be put around the spectrometer enclosure, to help damp the temperature variations outside and inside the enclosure.

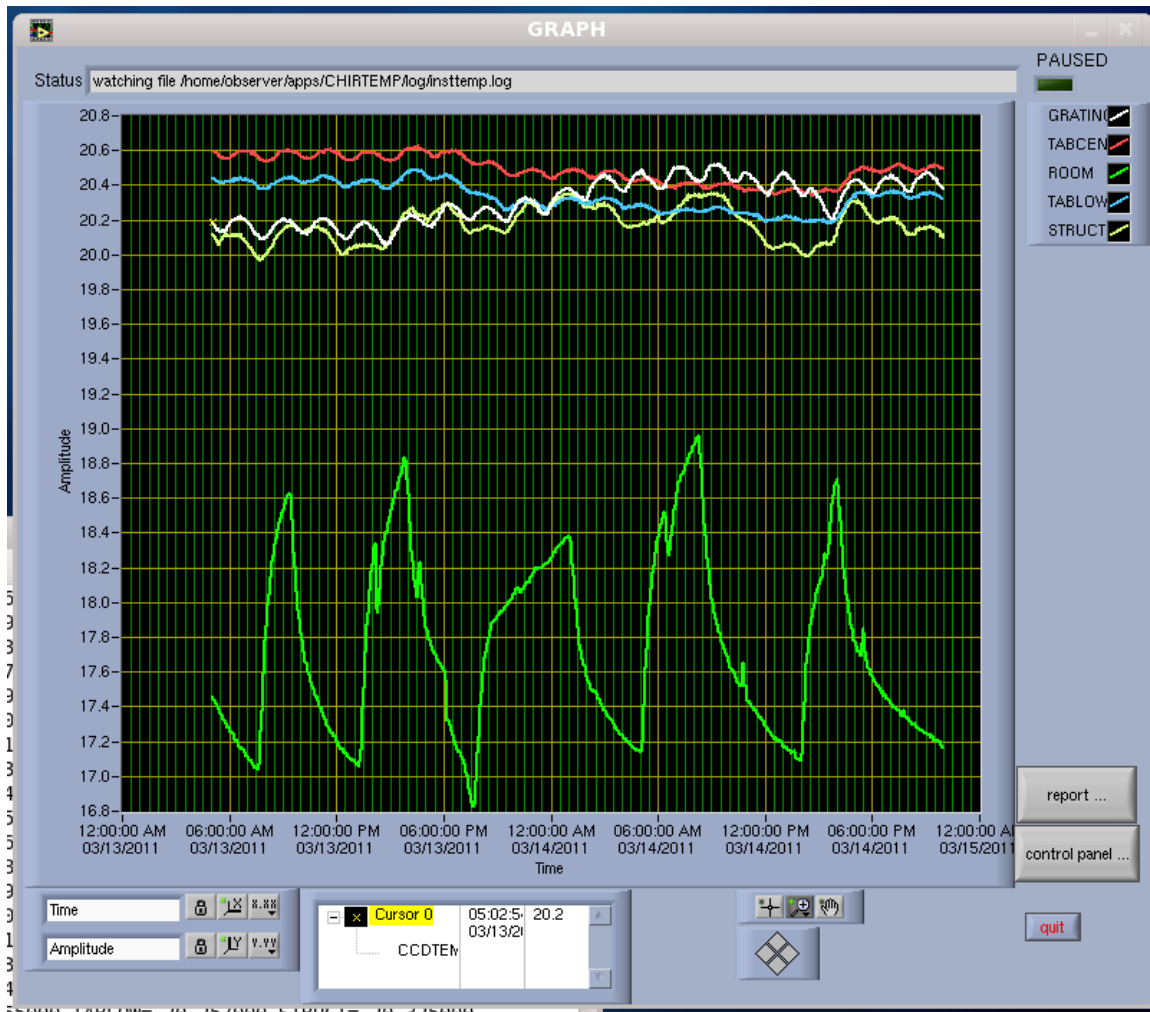


Figure 4. CHIRON temperature GUI shows temperature in the room (large amplitude temperature cycles) and inside the enclosure.

Resolution

The wavelength calibration program, *thid.pro*, returns a resolution, $R = dl / l$. This code has been used for more than a decade at Lick and Keck and the measured resolution is comparable to that obtained using iodine spectra. **Table 1** summarizes the resolution measurements:

TABLE 1: RESOLUTION			
Date	Obs num	Slit	Resolution
11-03-09	rqa31.0072	slicer	90,000
	rqa31.0102	slicer	90,000
	rqa31.0105	Fiber	30,400
	rqa31.0106	norm slit	87,900
	rqa31.0109	narrow slit	118,000
11-03-10	rqa31.1085	narrow slit	116,300
	rqa31.1090	narrow slit	123,200
	rqa31.1091	slit	89,500

	rqa31.1092	fiber	28,300
	rqa31.1094	fiber	23,500
11-03-11	rqa31.2266	fiber	28,300
	rqa31.2267	slit	88,900
	rqa31.2287	narrow slit	119,500
11-03-12	rqa31.3042	narrow slit - bad slicer position	92,000 ???
	rqa31.3043	narrow slit	123,500
	rqa31.3219	narrow slit	123,300
	rqa31.3220	narrow slit	125,300
11-03-13	rqa31.4031	slit	89,000
	rqa31.4032	slit	89,800
	rqa31.4034	Slit	89,000
	rqa31.4342	slit	89,000
	rqa31.4033	narrow slit	123,800
	rqa31.4343	Fiber	31,300
	rqa31.4344	Slicer	91,000

Throughput

Andrei Tokovinin carried out an analysis of the Canopus observations taken 9 Mar 2011 by extracting a wavelength segment near the center of the (left) chip. Comparing this with expected flux for a 0th magnitude star, he measured absolute efficiencies (**Table 2**).

TABLE 2: ABS EFFICIENCY	
Slit	Efficiency
Fiber	4.1 to 5.4 %
Slicer	2.9 to 3.6 %

TABLE 3: RELATIVE EFFICIENCY				
Observation number	slit	Continuum counts	Exposure time (s)	Counts per second
rqa31.4215	narrow	55,000	20	2.75
rqa31.4212	slit	38,000	7	5.43
rqa31.4213	slicer	80,000	7	11.4
rqa31.4214	fiber	50,000	3	16.7

We compare the relative efficiency of all four slits in **Table 3**. The ratio of the relative efficiency of the slit and fiber is identical to the ratio of Andrei's absolute efficiency measurements. The spectra used for this measurement were segments from template observations of alpha Cen A, from near the center of the detector (Order 20, pixels 1800:2500).

Figure 5 shows the normalized flux for narrow, slicer, slit and fiber observations. The spectrum extracted from the image slicer is clearly shifted relative to the other spectra. The slicer image is also shifted in the cross dispersion direction (discussed in the software section of this report). Since the narrow and regular slit are on a plate attached to the image slicer, it is not surprising that they are not exactly aligned with the slicer image.

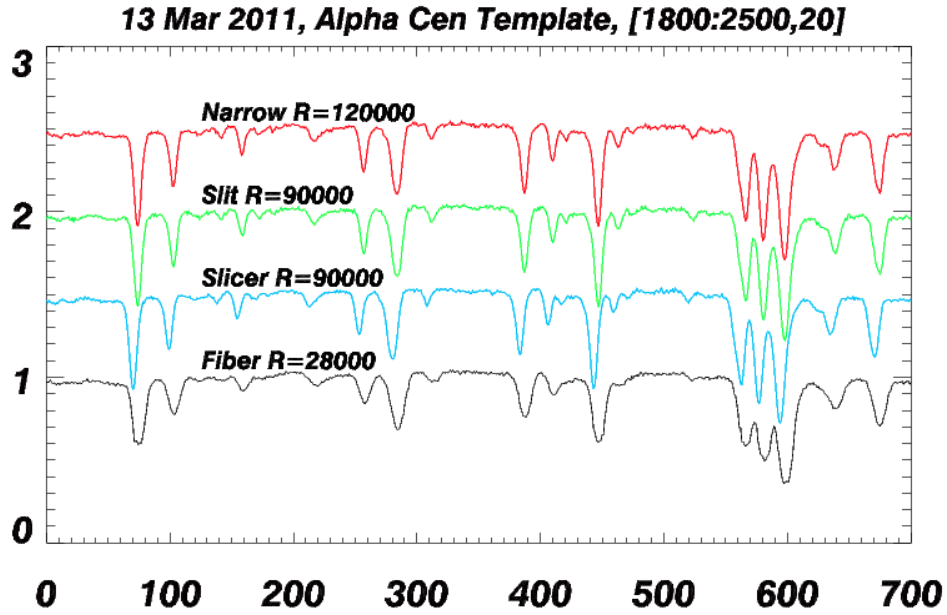


Figure 5. Normalized spectra of four (consecutive) alpha Cen observations, made with the different slits available with CHIRON. The continuum counts for these spectra are listed in Table 3.

We also suffer light losses from the iodine cell. The cell that we are using at CTIO has a relatively high column density (filled at VP temperature of 37C). **Figure 6** compares consecutive observations of the same B star with the same exposure time. Our plan is to replace this cell with a new cell with a lower column density of iodine.

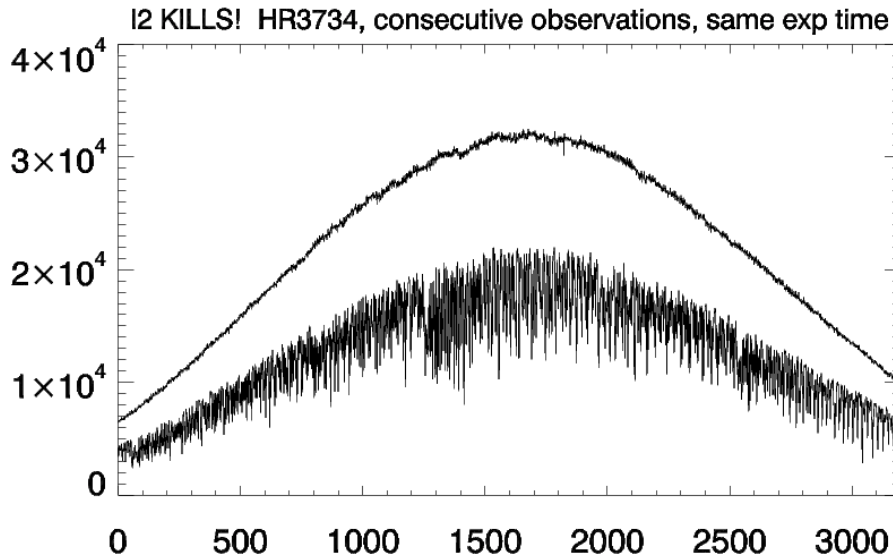


Figure 6. Two consecutive observations of the same B star, with and without iodine, showing significant light losses through the cell.

Stability

(foc.pro glitch, shake test)

We noticed a shift of the spectrum (1 pixel in the cross-dispersion direction) on the second day of the run. This can be seen in **Figure 7**, where a Gaussian fit to the cross-dispersion profile is shifted between a quartz observation taken at the beginning of night 1 and the next afternoon. Both observations were taken with the narrow slit and the cuts shown in **Figure 7** are identically made for the same mashed rows near the center of the chip. This shift was also picked up with *foc.pro* on different observations: thorium-argon images (narrow slit) also taken at the beginning of night 1 and the afternoon of night 2.

One concern was that this could be an issue with the controller. To check this, we show in **Figure 8** that the position of a bad column (pixel 606) on our detector did not shift; thus, this was not an issue with the controller or detector, but something in the spectrograph that moved between observations qa31.0037 (beginning of night 1) and qa31.1023 (afternoon before night 2). We continued to run *foc.pro* (with a static line list). No further shifts were observed on subsequent nights.

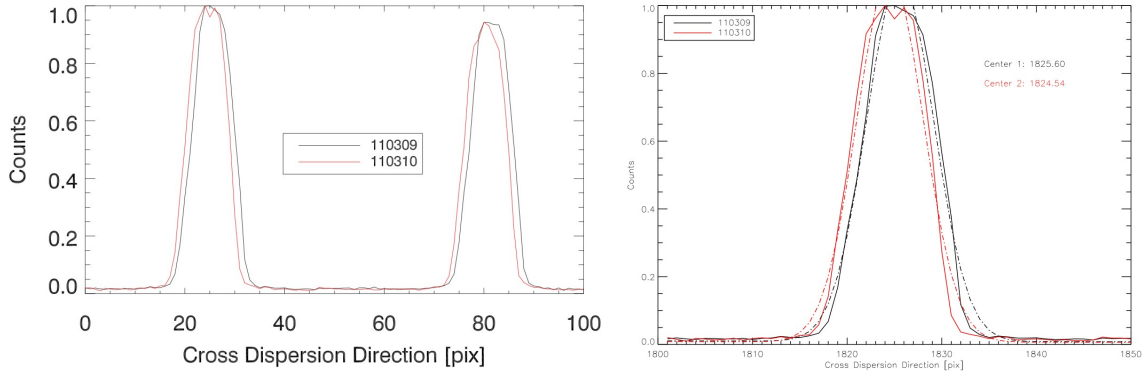


Figure 7. The cross-dispersion profile is fit with a Gaussian for two observations: qa31.0037 (red) and qa31.1023 (black). Both are quartz images, observed with the narrow slit. This figure shows a shift in the cross dispersion direction sometime during the first night or next day.

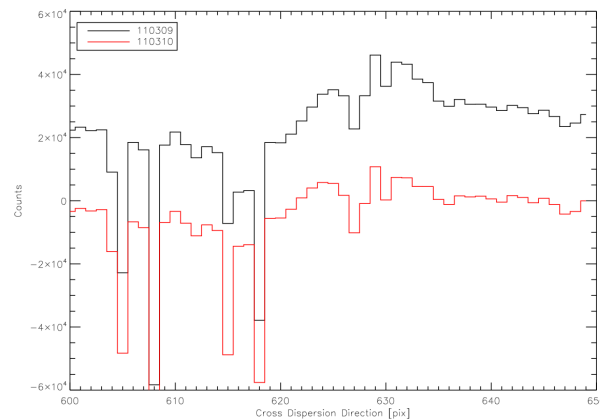


Figure 8. Flux from two exposures qa31.0037 (red) taken at the beginning and end of the first night, and qa31.1023 (black) taken the next afternoon. While the spectrum had shifted, the known bad column at pixel 606 did not shift, showing that this was not a problem with the electronics, but something that moved inside the spectrograph.

During the January commissioning run, we noticed that when the 1.5-m dome turns, the vibrations propagate to the Coude room. We saw this when a green laser on the FOB shook quite noticeably. Here, we attempted to check for the impact of vibrations on an exposure of a Bstar. We obtained six consecutive observations of the same Bstar (120 second exposures) with the iodine cell. For the first three observations, we observed normally (dome not tracking) and for the second three exposures we intentionally rotated the dome. There are two tests that we carried out to check the impact of vibrations on the spectrometer: (1) shifts of the iodine lines as evidenced by cross correlating spectra or (2) a change in the width of the modeled LSF.

We measured a shift of 0.0375 pixels for cross-correlated the Bstar (iodine) observations made with no rotation of the dome; the shift increased to 0.108 pixels for the observations with the dome rotating. This seems marginally significant; we compared the pixel shift for several other sets of consecutive Bstar observations.

We then compared the LSF model for those same six B stars. The three observations taken with the dome fixed are shown as black lines in **Figure 9** and the LSF models for the observations made while the dome was turning are shown as red lines. Again, there is a marginal difference between the two sets.

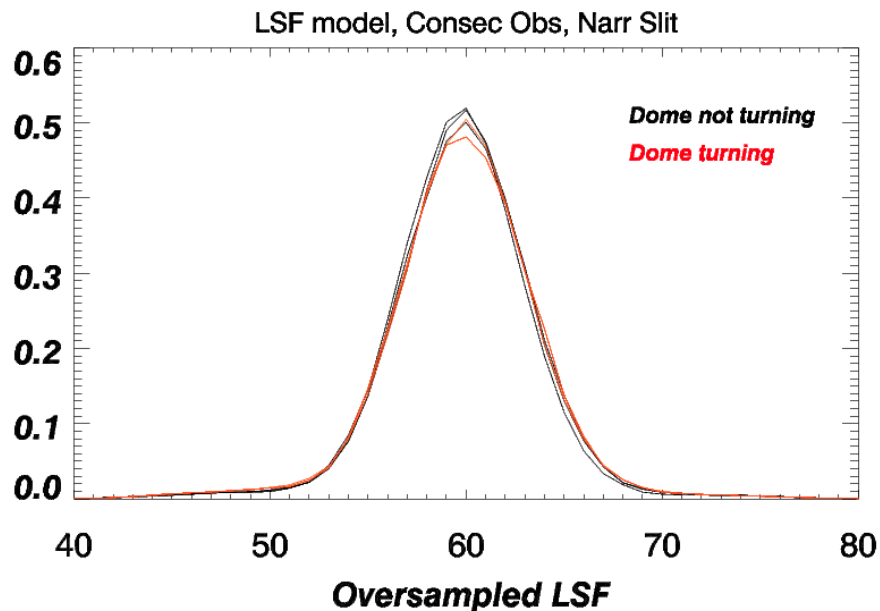


Figure 9. LSF model for B star iodine observations; three were taken with the dome fixed (black) and three with the dome turning (red).

Future work:

1. Monitor (how?) instrumental stability (check for shifts in the iodine or ThAr spectra)
2. Coude room environment: Fan, tent for CHIRON and O2 monitor
3. Monitor I2 cell temperature (record in FITS header and display on datataker (currently using the old controller which is not networked))
4. Exposure meter
5. Monitor (control?) pressure in CHIRON

Software Development

Current restrictions in our software include: dual amp, fast mode r/o, 3x1 binning.

The raw reduction code makes use of chip geometry recorded in the FITS headers and able to handle all both slits, the fiber and the slicer. However, it has not yet been generalized to switch between quad amp and dual amp mode. This is currently low priority since one configuration is adopted long term (and quad amp readout is not currently possible), however it is on our list of (lower) priority tasks to complete. It will be easy to handle slow readout (different read noise); however, this has not yet been implemented.

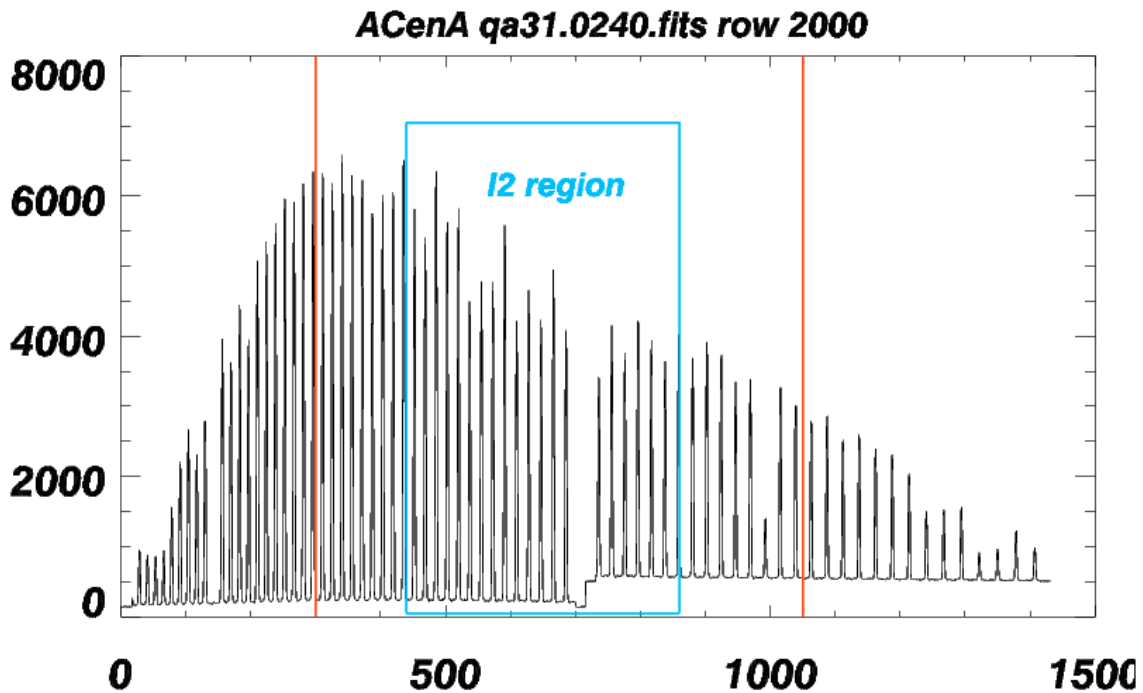


Figure 10. Red vertical lines indicate the orders that are extracted in our reduction code. The iodine region is safely included. While additional orders could be extracted, the signal decreases significantly outside of the selected borders at bluer and redder orders.

Logmaker program

This code was revised, and *logmaker.pro* now replaces *logmaker_widg.pro*. When all observations are in a given directory (e.g. “110309”), a logsheet will be generated listing those observations. Information about binning and the slit are extracted from the FITS header and are included as comments in the logsheet. Assumptions about directory paths are hardwired at the top of the program. The object name is read from the FITS header, however the keyword for the lamp (thar, quartz) and the iodine cell are used to override incorrect object names (for thar, quartz, iodine, only).

```
IDL> logmaker, '110309'
```

Extracting the spectra

It is important that the logsheet names are correct, since the logsheet is used to group (narrow, slicer, slit, fiber) observations with the correct calibrations (*sorting_hat.pro*).

```
IDL> sorting_hat, logsheet='110311',run='rqa31',/reduce,/narrow
```

The program also has an option that checks to be sure that for a given logsheet, all ThAr observations have been run and all spectra have been reduced and FITS formatted.

```
IDL> sorting_hat, logsheet='110311',run='rqa31',/end_check,/narrow
```

The raw reduction code, *reduce_ctio4k.pro*, extracts the spectra from the 2-D image. The usual process is followed: $(\text{object} - \text{bias}) / (\text{flats} - \text{bias})$, with a median bias subtracted row-by-row. Because we are using dual amp readout, the image is treated in two sections. The bias is subtracted from each section, a nonlinearity correction is made, and the gain is applied before concatenating the full image. The image is then rotated (so orders are along rows) and trimmed again as shown by the red lines in **Figure 10**.

When observing with a slit, flat fielding is carried out by using images observed with a decker that is taller than the cross dispersion width. This is not possible with fibers and CHIRON now has additional complexity with four slit settings: the fiber ($R \sim 30,000$), the image slicer ($R \sim 90,000$), a slit ($R \sim 90,000$) and a narrow slit ($R \sim 120,000$). **Figure 11** shows the cross dispersion profiles for these four slits. While it might be possible to use the fiber for flatfielding the slit spectra, there is enough of an offset that it seems better to take separate sets of quartz calibration images.

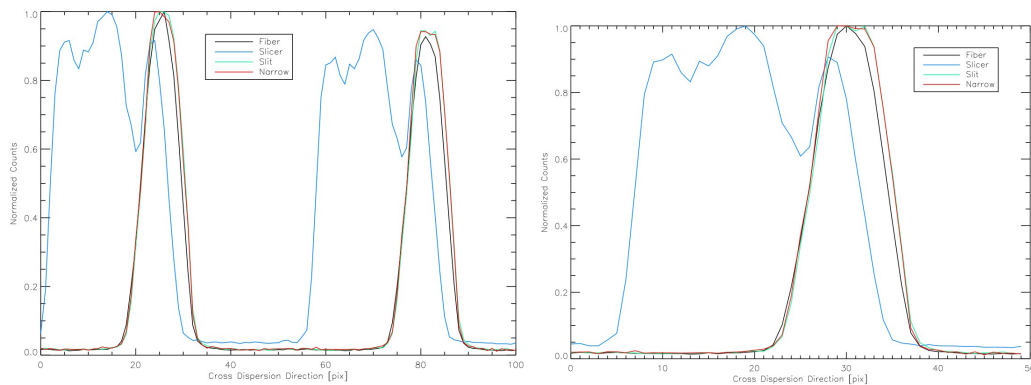


Figure 11: Cross dispersion profile for the fiber, slit, and narrow slit are nearly coincident. However the slicer image is broader (as expected) and offset from the slits.

Unfortunately, the added number of calibrations comes with some overhead. The ideal set of calibration images includes one ThAr, one quartz-illuminated iodine spectrum and 10 quartz images at the beginning and 10 at the end of the night (in case of drift, particularly important for the fiber). If there are four potential settings, then this is quite a burden for the telescope operator and observer. Matt Giguere developed a pan script for calibrations that is now included in the preset options: the *night_calib* will read the GUI (for the directory path, observer, sequence and file prefix name) and then make a new directory, obtain the full set of calibrations for all four slits and *rsync* the *ctioe1* (data) directory with *ctimac1*. A second preset option, *morning_calib*, will take the morning calibrations, *rsync* all files and launch the logmaker program.

The flatfield is produced in two stages. First, the quartz images are coadded (median for each pixel) to produce a *total_flat*. A second version of *total_flat* is created by median smoothing in

the x-disp direction. The total flat is then divided by the smoothed surface so that the pixel-to-pixel variations are maintained, but low frequency patterns are removed.

Cosmic ray removal is carried out on the raw (2-D) image and is based on the optimal extraction of Valenti & Piskunov. The echelle orders are fit with a slit function and pixels that spike above the surface are replaced. However, this code has not been optimized for slit observations and this remains an issue that merits further investigation.

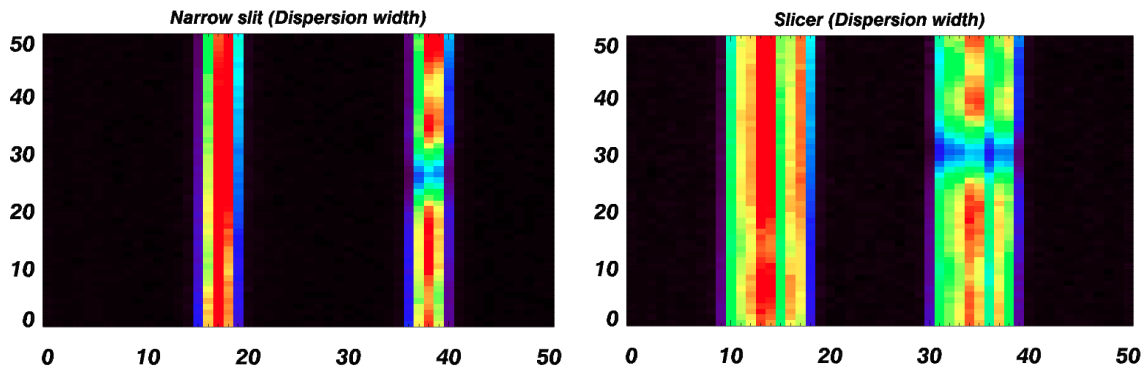


Figure 12. Observations are shown for the 3x1 binned narrow slit and the 3x1 binned image slicer. To extract the spectra, the order width must be defined. Here, widths are set to 6 pixels for the narrow slit and 12 pixels for image slicer to extract all light.

The order locations and widths must be found in order to extract the 1-D spectrum. Swaths (about 20 pixels wide) stripe the image format in the *cross-dispersion* direction. The peak flux in the swaths then locates the center of each order. The peaks are fit with a polynomial, which traces the arc of the echelle order. Once the peak of each order has been found, the width for extraction is defined. The `reduce_ctio4k` code takes `xwid` as input. **Figure 12** shows the cross dispersion width for 3x1 binning with the narrow slit and the slicer image. Based on this, we adopt `xwid=6` for the fiber and slits and `xwid=12` for the image slicer. Pixel columns are mashed within $\pm xwid / 2$. This gives a single flux for each pixel in the order. Traced orders that run off the edge of the chip are not extracted (e.g., orders at the top or bottom of the CCD image).

Wavelength calibration:

Wavelength calibration is carried out with the IDL program, *thid.pro*. The wavelength solution is a 2-d polynomial fit and a wavelength array that is identical in size and form to the extracted spectral orders is saved and written along with the spectrum to a single (FITS) file. Reduced spectra can be found on `ctimac1` in `/mir7/`

Future tasks:

1. Provide logic to handle other binning configurations (low priority)
2. Complete a top-level driver program that operates at CTIO and reduces all spectra and runs thorium-argon wavelength calibration code in a single call (pass only the nightly directory '110309' and the run tag 'rqa31') and then generates the wavelength calibrated FITS files (high priority).
3. Unify the number of extracted orders; currently either 40 or 41 orders are extracted

- (high priority).
4. Non-linearity coefficients should be used to correct at the stage of bias
 5. Optimize cosmic ray handling
 6. Automatic determination and handling of amplifier mode (low priority)

Science Tests

The Doppler analysis is carried out by analyzing chunks of the spectrum (80 pixels, or about 2 Angstroms wide). An FTS iodine observation was convolved with a model PSF (17 PSF parameters are free parameters in a Levenberg-Marquardt algorithm) to fit observations of Bstars made with CHIRON. The reduced χ^2 fits were typically close to 1.0, however seven of 684 chunks had chisq fits worse than 2.0 (396:20.1, 477:2.92, 500:14.9, 607:7.0, 610:8.4, 613:3.76, 626:2.96) and should be checked (bad column?) and masked out.

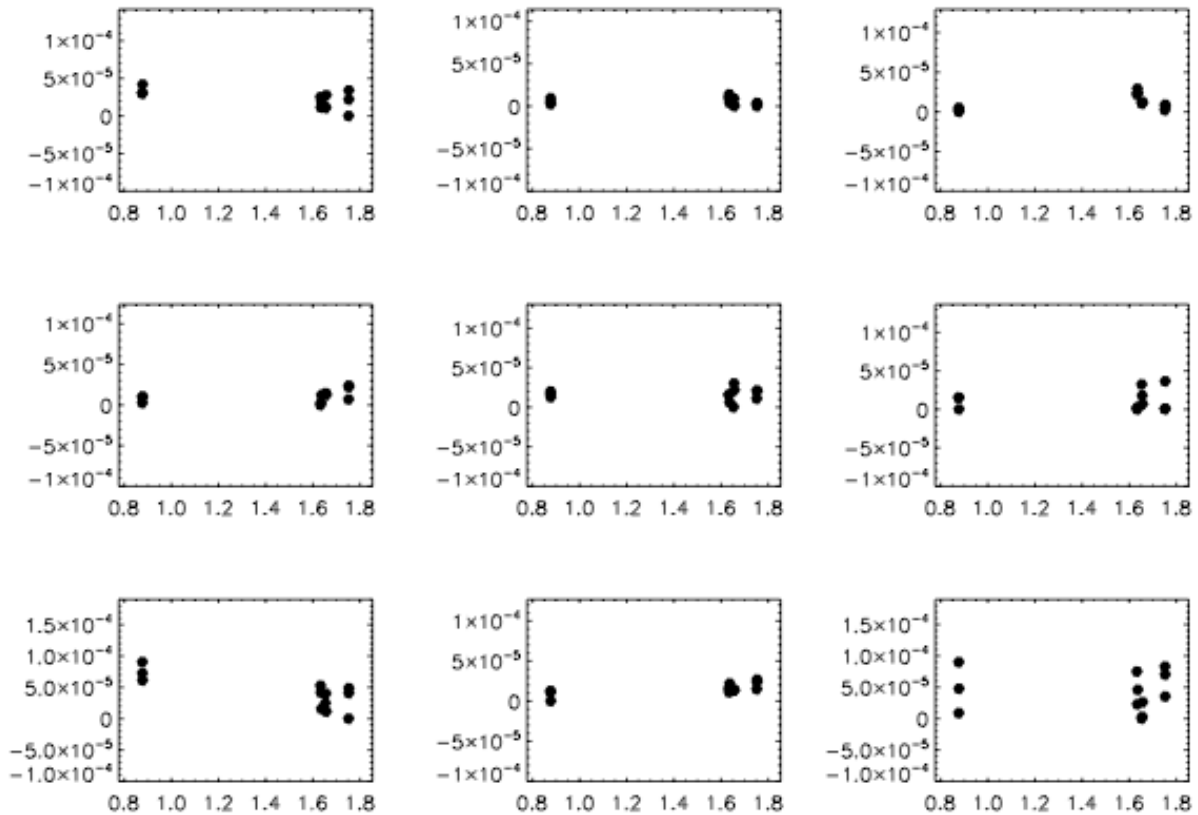


Figure 13. For nine wavelength segments (chunks) extracted from locations on the 2-D CCD as represented above (upper left, upper middle, upper right, middle left, middle, middle right, lower left, lower middle, lower right; each row above is extracted from a single top, middle, bottom order), differences in the dispersion solution for the chunk are plotted as a function of time (in days). Since the dispersion should not be changing, these may represent errors in the model.

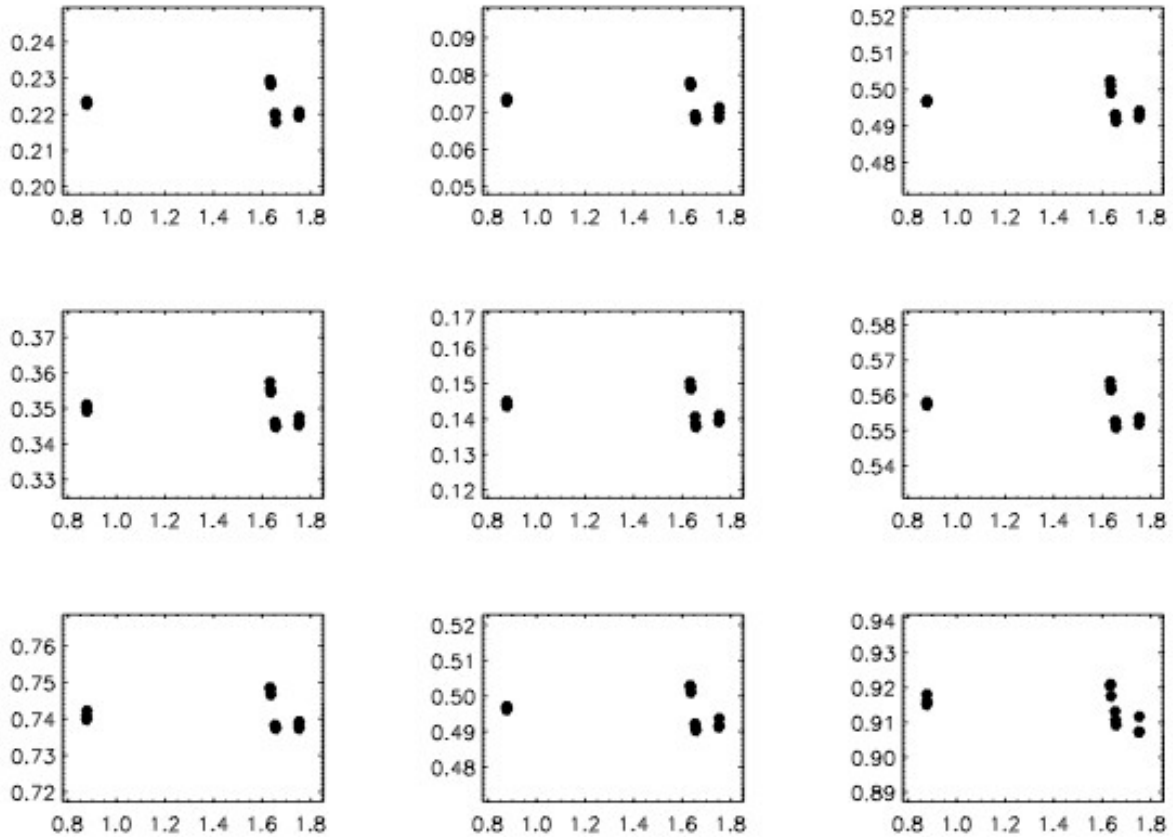


Figure 14. For the same chunks shown in Figure 13, differences in the wavelength solution for the first pixel of the chunk are shown. For consecutive observations, the wavelength differences are small (as expected) and the larger shifts might be caused by pressure changes inside the spectrometer. Since this is an iodine solution, the barycentric velocity is irrelevant.

Models of the iodine fits were examined and some results are shown for selected 80-pixel chunks in Figures 13 – 15. In these figures, the top row of chunks was extracted from order 13; the middle row of chunks was selected from order 21 and the bottom row is from order 28 and the same chunks are shown (80-pixel chunks beginning with 240 on the left, 1520 in the middle and 2880 on the right). The data sets are taken from two different nights.

In Figure 13, differences in dispersion are compared for each observation and plotted as individual dispersions minus the dispersion from the first observation and plotted vs $JD - \min(JD)$. The RMS of the dispersion changes over time is of order 10^{-5} . The dispersion is expected to be constant (to what level?) and certainly constant for consecutive observations. So, the observed scatter could be errors in modeling (that translate to errors in radial velocity).

In Figure 14, a similar check is made for the model wavelength solution. The y-axis shows the difference between w_0 (wavelength of the first pixel in the chunk) for the first observation and subsequent observations in Angstroms. Consecutive observations have wavelength differences that are less than the plot scale (less than 0.002 Angstroms, which is still as much as $1/10^{\text{th}}$ of a pixel) but there are shifts between blocks of observations that may reflect pressure changes in the spectrograph (which cause the spectrum to shift on the detector).

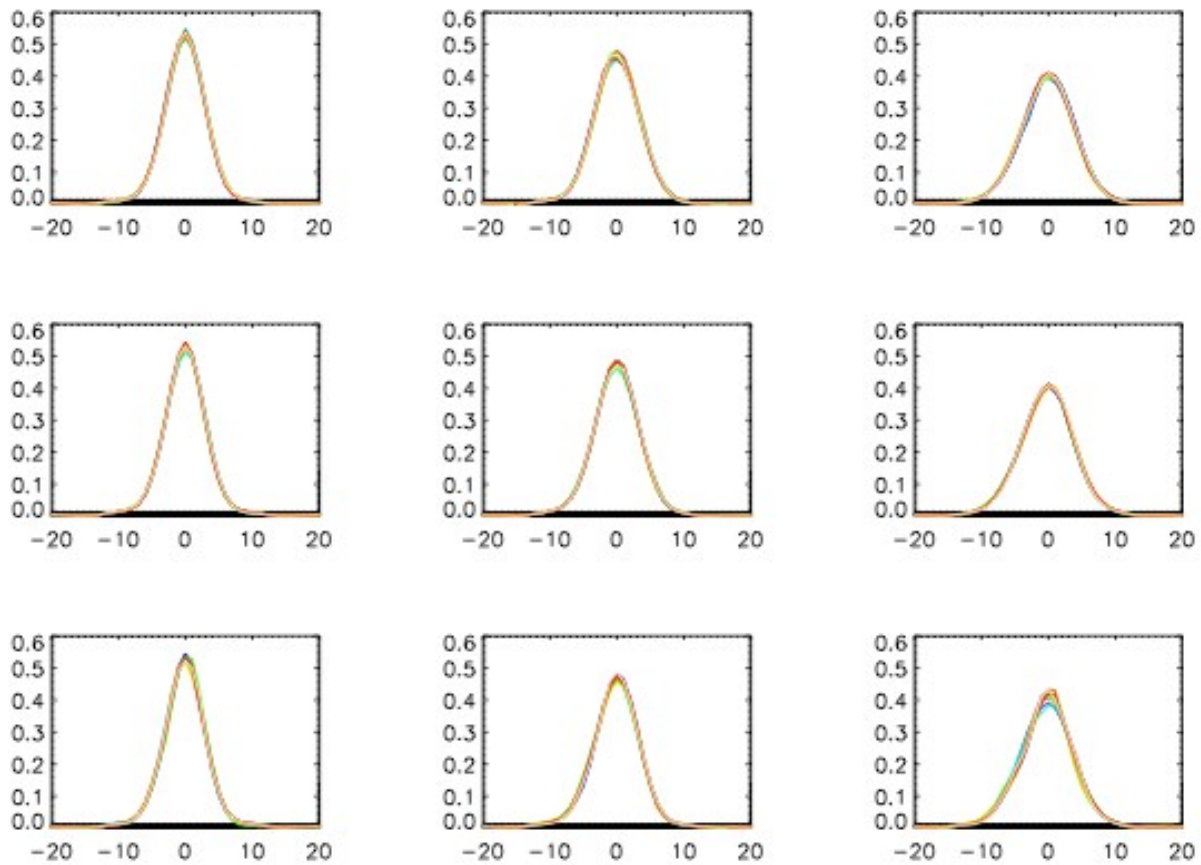


Figure 15. For the same chunks as Figure 13 and 14, the PSF models are overplotted.

In Figure 15, the PSF models are shown for the same chunks. Two trends are seen: the PSF becomes wider going from left to right across the detector (true for all orders, not just the ones shown here). It is not clear why this would happen if the CCD is not tilted w.r.t. the incoming light. However, this trend is consistent with a slight slope seen when the FWHM was plotted during focusing.

To simplify the initial Doppler analysis, only the data observed with the narrow slit were analyzed for alpha Cen A. Twenty consecutive “template” observations (no iodine) were shifted (cross-correlated), coadded and then deconvolved to generate an intrinsic stellar spectrum (ISS) for alpha Cen A. This ISS was used to analyze 134 observations of alpha Cen A taken on three nights. The velocity dispersion for all of the (unbinned) data was 2.63 ms^{-1} .

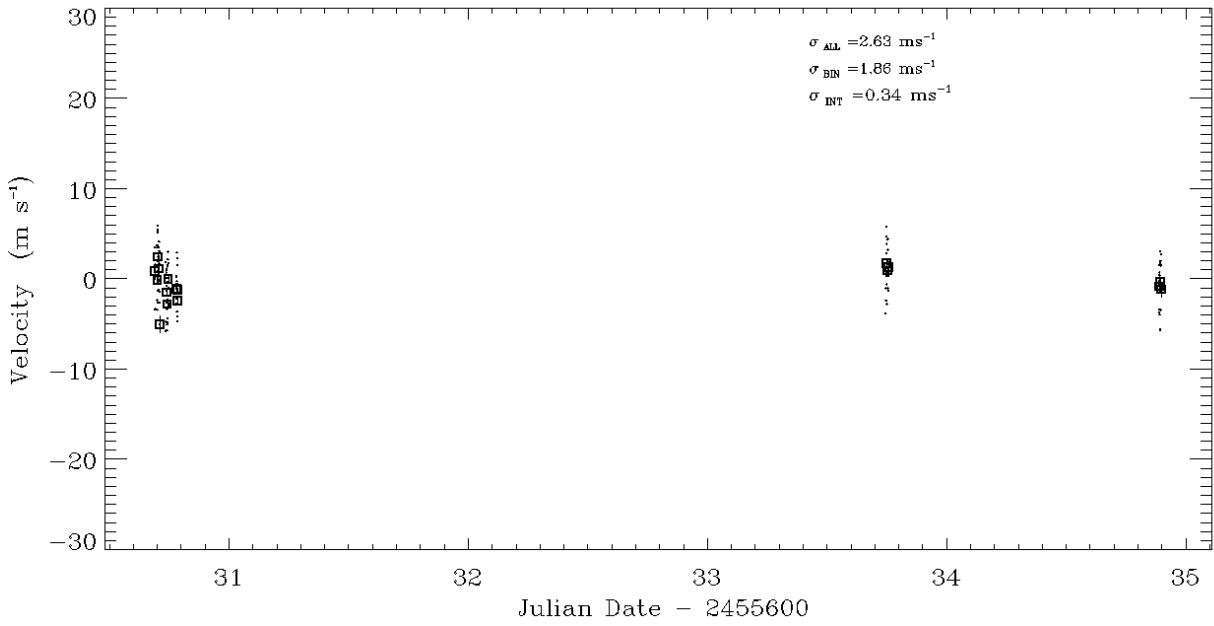


Figure 16. 134 unbinned RV's taken over three nights (with the narrow slit) have a standard deviation of 2.63 m/s. Most of the data and

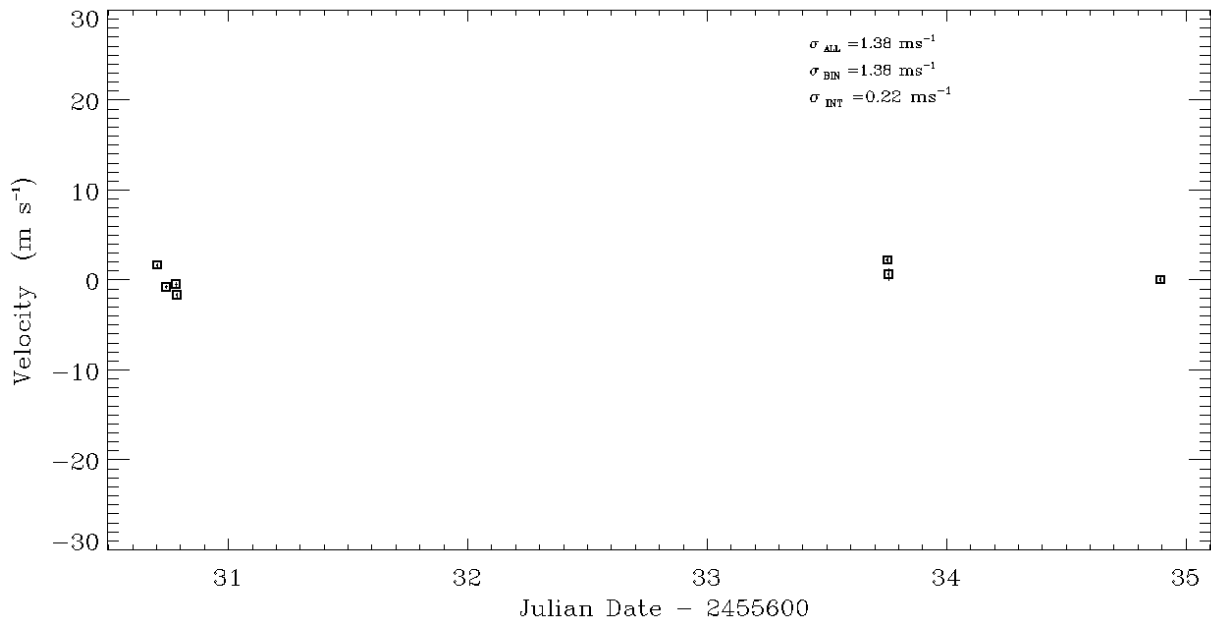


Figure 17. When the velocities shown in Figure 16 are binned by 1 hour, the RMS for all of the data drops to 1.38 m/s. The formal error is unrealistically small for these binned data at 0.22 m/s.

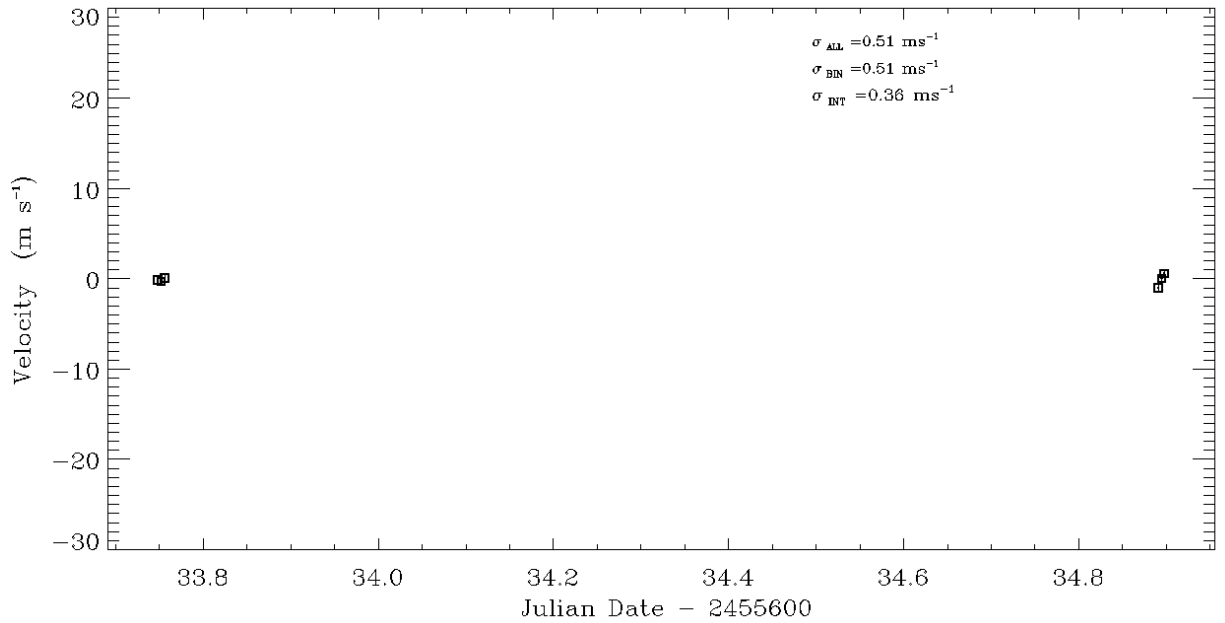


Figure 18. When the last two nights of data shown in Figure 16 and 17 are binned by 5 minutes, the standard deviation is 0.51 ms^{-1} and the binned errors are 0.36 ms^{-1} .

We still have small numbers (only three nights run) with about 30 observations per night (more on the first night). However, the preliminary analysis shows that CHIRON should achieve better than 1 m s^{-1} precision.